Electronic Supplementary Information

Morphological Transition and Transformation of 2D Nanosheets by Controlling Balance of π−π Stacking Interaction and Crystalline Driven Force

Heng Li,[#] Liang Han,[#] Yulin Zhu, Nan Zheng, Hanjian Lai, Paco Fernández-Trillo and Feng He*

H. Li, L. Han, Y. L. Zhu, H. J. Lai, Prof. F. He
Shenzhen Grubbs Institute and Department of Chemistry, Southern University of Science and Technology, Shenzhen, 518055, China
E-mail: hef@sustech.edu.cn

H. Li, P. Fernández-Trillo,
School of Chemistry, University of Birmingham, B15 2TT, UK

P. Fernández-Trillo
Departamento de Química, Facultade de Ciencias and Centro de Investigacións Científicas Avanzadas (CICA), Universidade da Coruña A Coruña, 15071, Spain

Dr. N. Zheng
Institute of Polymer Optoelectronic Materials and Devices, State Key Laboratory of Luminescent Materials and Devices, South China University of Technology, Guangzhou, 510640, China

Prof. F. He
Guangdong Provincial Key Laboratory of Catalysis, Southern University of Science and Technology, Shenzhen, 518055, China

Supplementary Methods

1. Experimental Methods

Materials. Most of reagents and solutions were used as commercially received in synthesized procedures except dimethylformamide (DMF), potassium tert-butoxide (K*t*BuO), 1,1-diphenylethlene (DPE), 2-vinylpyridine (2VP), lithium chloride (LiCl), tetrahydrofuran (THF) and benzene. DMF was dried with molecular sieve before used. K*t*BuO and LiCl were heated at 120 °C under vacuum to remove water. DPE was titrated with n-BuLi until a red color sustained and then distilled under reduced pressure. 2VP was distilled with CaH_2 twice. THF and benzene was dried with Na and used as freshly distilled.

Characterization Equipment. ^{1}H NMR spectra were measured on a Bruker AVANCE 400 MHz spectrometer with tetramethylsilane (TMS) as the internal standard. Molecular weights were determined by GPC measurements, which were carried out on a Waters ACQUITY APC System equipped with a UV detector (Waters ACQUITY TUV) and 3 series connected chromatographic columns (ACQUITY APC XT 450, 200, 45, 4.6 × 150 mm). Polystyrene standards (Aldrich) were used for calibration, and THF was used as the eluent with a flow rate of 0.5 ml min^{-1} at 40 °C.

Transmission electron microscopy. Transmission electron microscopy (TEM) photographs were taken by using a Hitachi HT7700 TEM instrument and operating at 100 kV. The samples were prepared by putting a drop of solution of assemblies on carbon-coated copper grids followed by solvent evaporated. For the statistical analysis, the achieved photos were analyzed by using Digital Micrograph software package

developed by the US Gatan company. The diagonal length was used to characterize the scale of the 2D rectangular micelles. The number-average length (L_n), the weight-average length (L_w), the number-average width (W_n), the number-average diameter (D_n), the weight-average diameter (D_w) and the weight-average width (W_w) of the 1D or 2D micelles were calculated by the following equations: (where L_i and W_i are the sizes of individual 1D or 2D micelles, respectively, N_i are the number of L_i and W_i).

$$L_n = \frac{\sum_{i=1}^{N} N_i L_i}{\sum_{i=1}^{N} N_i} \qquad (Equation\ S1)$$

$$L_w = \frac{\sum_{i=1}^{N} N_i L_i^2}{\sum_{i=1}^{N} N_i L_i} \qquad (Equation\ S2)$$

$$W_n = \frac{\sum_{i=1}^{N} N_i W_i}{\sum_{i=1}^{N} N_i} \qquad (Equation\ S3)$$

$$W_w = \frac{\sum_{i=1}^{N} N_i W_i^2}{\sum_{i=1}^{N} N_i W_i} \qquad (Equation\ S4)$$

$$D_n = \frac{\sum_{i=1}^{N} N_i D_i}{\sum_{i=1}^{N} N_i} \qquad (Equation\ S5)$$

$$D_w = \frac{\sum\limits_{i=1}^{N} N_i D_i^2}{\sum\limits_{i=1}^{N} N_i D_i} \qquad (Equation\ S6)$$

Atomic force microscopy. The detected AFM samples were prepared by drop-coating about 15 μL of the 2-D assemblies' solution onto a pre-cleaned and treated silicon wafer followed by evaporating the solvent isopropanol. The silicon wafers used as substrate were cleaned in piranha solution for 6 h, then ultrasound treated in ethanol, water, and ultrapure water in turn, and finally dried with blowing nitrogen. The images were gained using an Asylum Research AFM in AC mode under ambient conditions. The used sensor cantilevers were Silicon probe reflex coated with aluminum manufactured by Budget sensors Company. Images were analyzed with IGOR Pro software developed by WaveMetrics Inc.

Laser scanning confocal microscopy (LSCM). LSCM images were performed using a ZEISS LSM 900 inverted epifluorescence microscope with a × 63 (numerical aperture1.4) oil-immersion objective lens. A drop of sample solution of micelles was put on a cleaned slide followed sealing with a cover slip, which was prepared for observing. The samples of formed micelles in solution were excited using an argon laser operating at 405 and 488 nm and the confocal images were obtained using digital detectors with observation windows of 530–630 nm.

UV-Vis Absorption Spectra (UV-Vis). UV-Vis absorption spectra were recorded by a SHMADZU UV-3600. A capped cuvette containing an isopropanol solution of PPV-TIPS-b-P2VP$_n$ was placed in a spectrophotometer holder attached to a temperature

controller. The solution in the capped cuvette was heated to 80°C and kept for 2 h. The solution was then slowly cooled to room temperature. The UV-visible spectrum was recorded every 20 °C during the cooling process. After the sample solution was cooled to room temperature, it was recorded once at 24 h, 48 h and 72 h.

Grazing Incidence Wide-angle X-ray Scattering (GIWAXS). The samples were prepared by drop-coating 60 μl of the solution onto the pre-cleaned and treated silicon wafer followed by evaporating the solvent for seven times. The silicon wafers were cleaned in piranha solution for 30 min, then ultrasound successively in ethanol, ultrapure water, and finally dried with blowing nitrogen dispersed.

Differential Scanning Calorimetry (DSC). Different scanning calorimetry (DSC) measurements were performed on a Discovery series thermal analyzer at a scanning rate of 10 °C min-1 in N2 atmosphere. The samples were heated from 30 to 150 °C, and then cooled back to 30 °C. The thermal cycles carried on twice, and the data of second cycle were used to analyze. We employed the DSC to test the homopolymer in the solid state of PPV-EH and PPV-TIPS.

Computational methods. The ground state geometries were fully optimized by the DFT method with the Becke three-parameter hybrid exchange and the Lee-Yang-Parr correlation functional (B3LYP) and 6-31G* basis set using the Gaussian 09 software package.

2. Polymer Synthesis and Characterization.

All of air- or moisture-sensitive reactions were carried out in dried glassware under an argon pressure using Schlenk techniques or in a glove box under nitrogen atmosphere. The detailed procedure path of synthesis was illustrated in Scheme S1.
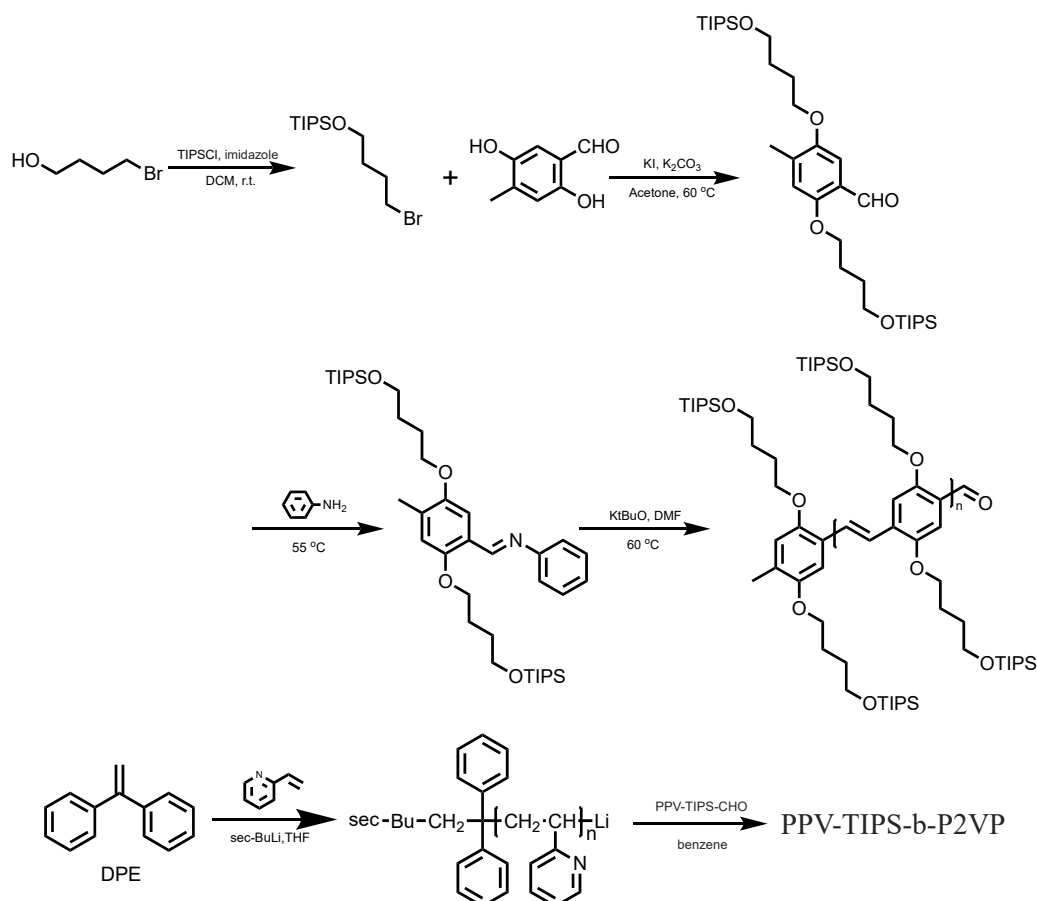

Scheme S1. Schematic synthesis route for PPV-TIPS-b-P2VP.

Synthesis of (4-bromobutoxy) triisopropylsilane (1). A mixture of 4-bromo-1-butanol (14.2 g, 37 mmol), chlorotriisopropylsilane (4.82 g, 25 mmol) and imidazole (1g, 14.6 mmol) in DCM (50 mL) was refluxed at room temperature overnight under Ar atmosphere. Then 100 mL water was added into mixture. The mixture was extracted with anhydrous EtOAc (3 × 40 mL), then the gathered organic phase was dried with MgSO$_4$, finally the solvent was removed by rotary evaporator. After purification by

chromatography (silica gel, petroleum ether), a yellow oil (**1**, 7.3 g, 0.023 mol, 94%) was obtained. ^{1}H NMR (400 MHz, CDCl$_3$): δ3.80-3.75 (t, 2H), 3.50 (t, 2H), 2.07-1.98 (m, 2H), 1.76-1.69 (m, 2H), 1.20-1.01 (m, 21H).
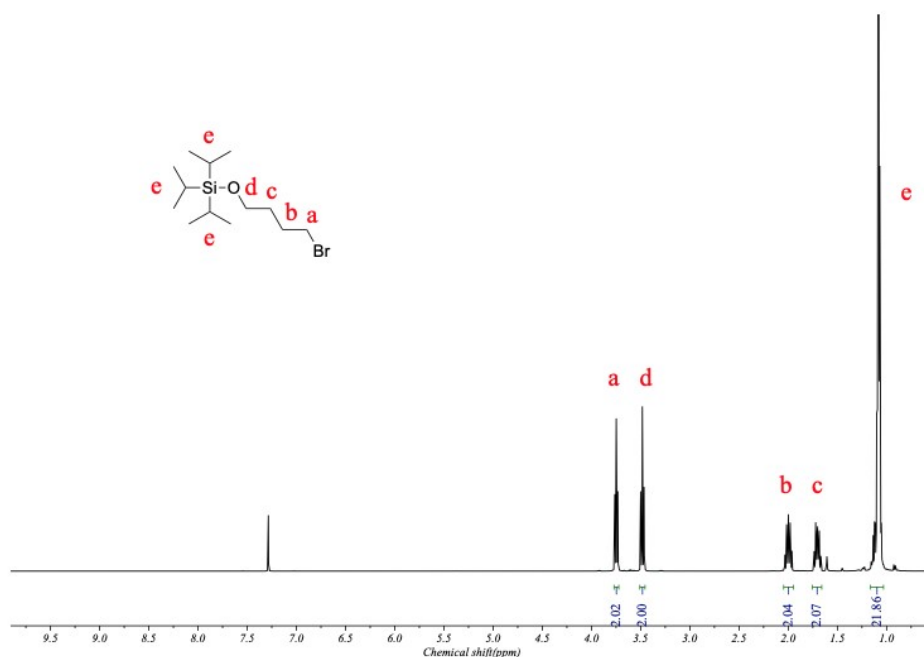
Figure S1. ^{1}H NMR spectra of (4-bromobutoxy) triisopropylsilane in CDCl$_3$.

Synthesis of 4-methyl-2,5-bis(4-((triisopropylsilyl) oxy) butoxy) benzaldehyde (2).

(4-bromobutoxy) triisopropylsilane (5.5g, 17.8 mmol) was dissolved in acetone (60 mL), then added K$_2$CO$_3$ (4.14g, 30 mmol), KI (1.24g, 7.5 mmol), and 2,5-dihydroxy-4-methylbenzaldehyde (912 mg, 6 mmol). The reaction was refluxed overnight. After cooling to room temperature, 60 mL water was added into mixture. The mixture was extracted with anhydrous EtOAc (3 × 50 mL). After dried by MgSO$_4$ and rotary evaporating, the obtained crude oil was purified by chromatography (silica gel, petroleum ether/ EtOAc 50:1), a white oil (**3**, 1.3g, 2.13 mmol, 35.6%) was obtained.

^{1}H NMR (400 MHz, CD$_2$Cl$_2$): δ 10.43 (s, 1H), 7.24 (s, 1H), 6.81 (s, 1H), 4.08 (t, 2H), 4.01 (t, 2H), 3.79 (m, 4H), 2.30 (s, 1H), 1.97-1.86 (m, 4H), 1.79-1.70 (m, 4H), 1.17-1.03 (m, 42H).
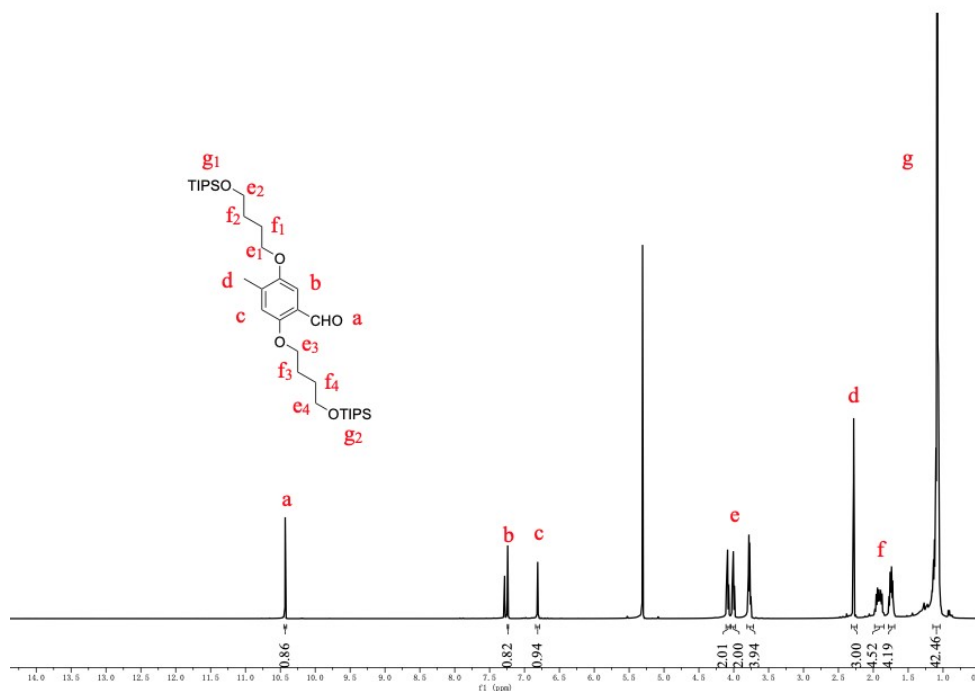
Figure S2. ^{1}H NMR spectra of 4-methyl-2,5-bis(4-((triisopropylsilyl) oxy) butoxy) benzaldehyde in CD$_2$Cl$_2$.

Synthesis of Poly-4-(5-chloro-2-((2-ethylhexyl) oxy)-4-methylstyryl)-2,5-bis((2-ethylhexyl) oxy))-benzaldehyde (PPV-TIPS-CHO) (3). A mixture of 4-methyl-2,5-bis(4-((triisopropylsilyl) oxy) butoxy) benzaldehyde (608 mg, 10 mmol) and aniline (6.16 g, 66.06 mmol) was stirred for 2h at 50 °C under reduced pressure, then the temperature of the mixture raised to 110 °C to remove excess aniline to yield red brown viscous oil. Next, the solution of oil in 15 mL anhydrous DMF was added into round flask containing potassium tert-butoxide (225 mg, 3 mmol) with 15 mL anhydrous

DMF at 50 °C. After stirring for 2h at the same temperature, the mixture was poured into 100 mL 1M hydrochloric acid and stirred for 48 h. Then the reaction mixture was extracted with chloroform (3 × 10 mL), and the organic phase was successively washed by aqueous $NaHCO_3$ and water followed by dried with $MgSO_4$ and rotary evaporating. Product in low dispersity was successively collected and fractionated by methanol, acetone and hexane with Soxhlet extraction. After Soxhlet extraction, we had purified the product by chromatography (silica gel, CH_2Cl_2: petroleum ether=1:3). Then, we used the high-performance liquid chromatography (HPLC) to further purify the product PPV-TIPS homopolymer. The value of Mn = 2540 and the polydispersity index was measured at 1.07 by GPC in THF. The number-average degree of polymerization n = 5 for PPV-TIPS-CHO was determined by GPC and ^{1}H NMR.
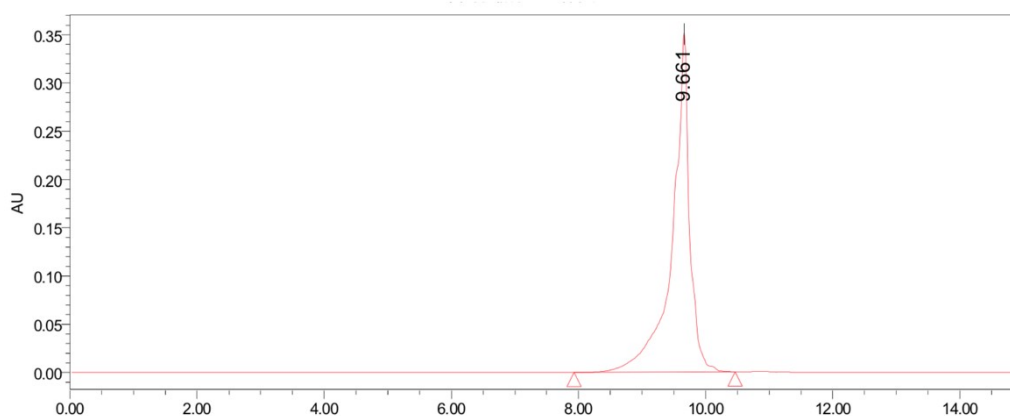
Figure S3. GPC traces of PPV-TIPS-CHO.

Table S1 Summary of the data of GPC of PPV$_n$-TIPS-CHO

Polymers	M_n	M_w	PDI	Retention time (min)
PPV$_5$-TIPS-CHO	2540	2722	1.07	9.661
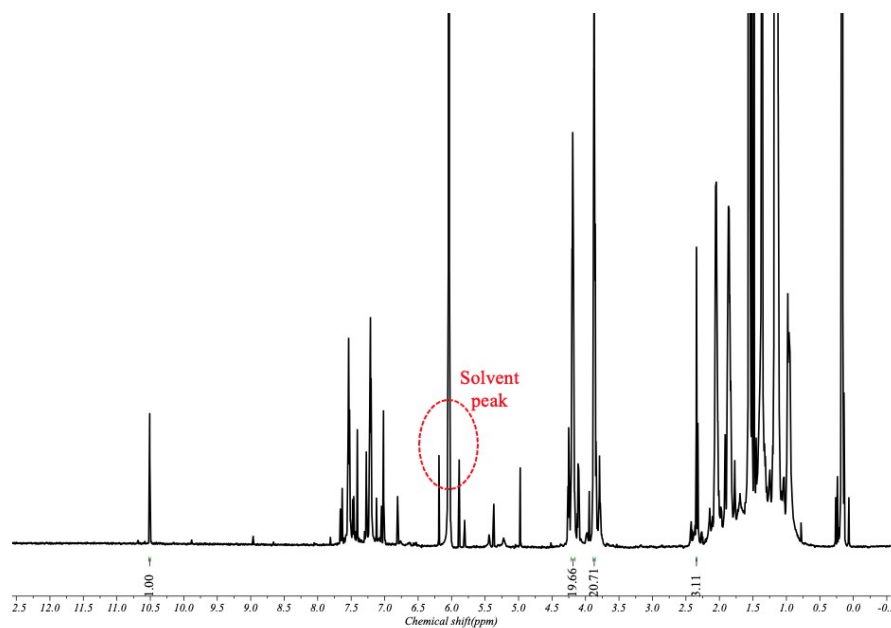
Figure S4. ^{1}H NMR spectra of PPV$_5$-TIPS-CHO in C$_2$D$_2$Cl$_4$.
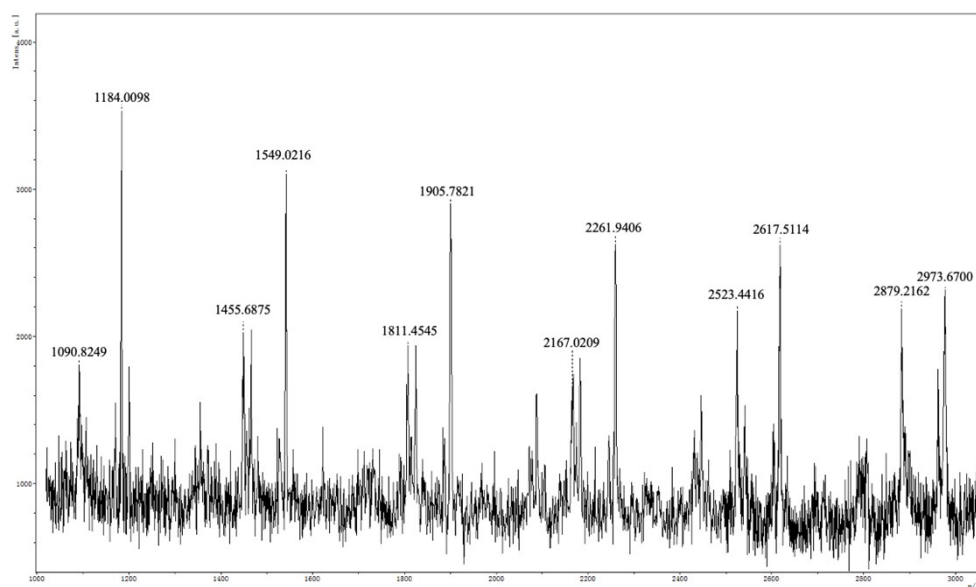

Figure S5. MALDI-TOF mass spectrum of PPV-TIPS-CHO. The PPV-core repeat unit

is 356 m/z and molecular weight of partial side chain unit (C$_5$H$_6$Si) is 94 m/z.

Synthesis of Poly(2,5-di(2'-ethylhexyloxy)-1,4-phenylenevinylene)-block-poly (2-vinylpyridine) (4, PPV-TIPS-*b*-P2VP). In a glovebox filled with N_2 at -78 °C, 86.9 µL of sec-BuLi (1.3 M in hexane) was quickly added to a stirring solution of dried LiCl (45.7 mg, 1.13 mmol) and 1,1-diphenylethylene (DPE, 20 µL, 0.113 mmol) in THF (2 mL). Then maintaining -78 °C, a certain amount of 2-vinylpyridine (2VP) in THF (2 mL) was added to the mixture. After the reaction went on running for 2h at -78 °C, a solution of PPV-TIPS-CHO (40 mg, 0.01mmol) in benzene (2 mL) was quickly added into the reaction mixture to quench the anion polymerization. Then the reaction temperature was increased to room temperature and stirred for additional 12 h. As the reaction stopped, the reaction mixture was poured into 25 mL chloroform and washed successively with aqueous HCl (pH = 3), water and aqueous $NaHCO_3$. After rotary evaporating, the crude residue was purified by chromatography (silica gel, eluent was changed from chloroform to chloroform/methanol = 10:1), and finally red solid was obtained. The block ratio of produced PPV_5-TIPS-*b*-$P2VP_n$ was determined by NMR and GPC.
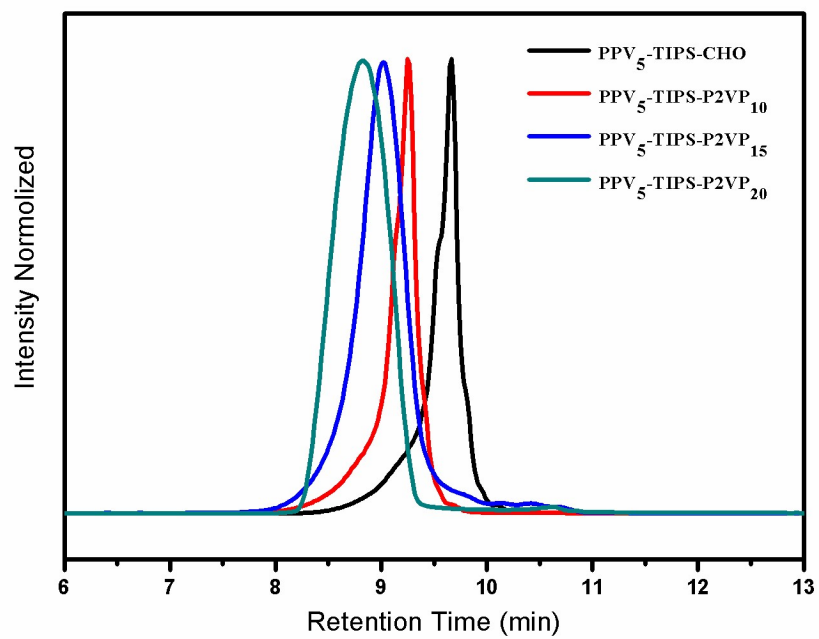
Figure S6. GPC traces (UV-Vis) of PPV$_5$-TIPS-*b*-P2VP$_n$.
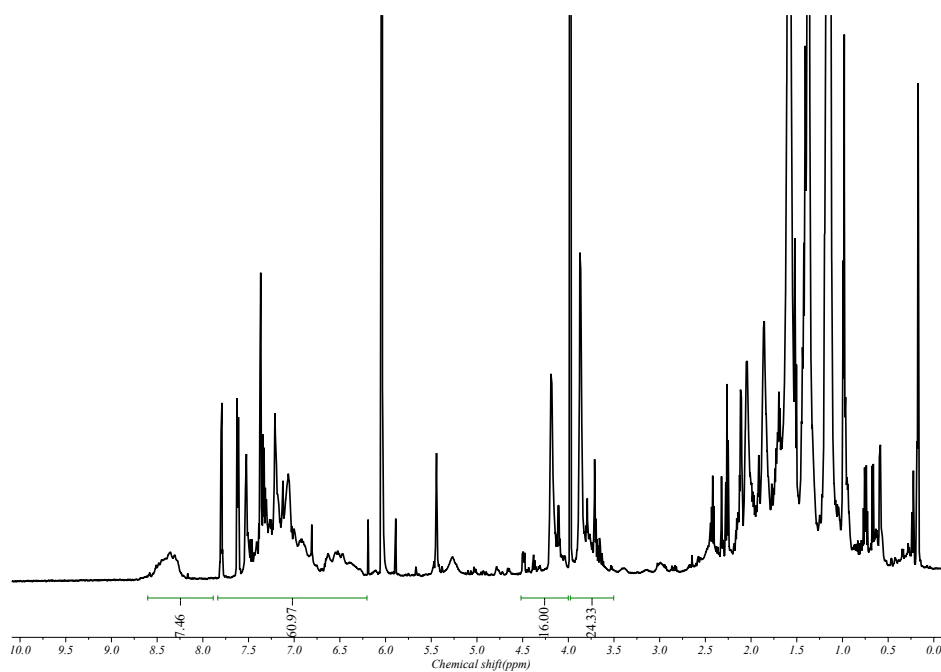
Figure S7. ^{1}H NMR spectra of PPV$_5$-TIPS-*b*-P2VP$_{10}$ in C$_2$D$_2$Cl$_4$.
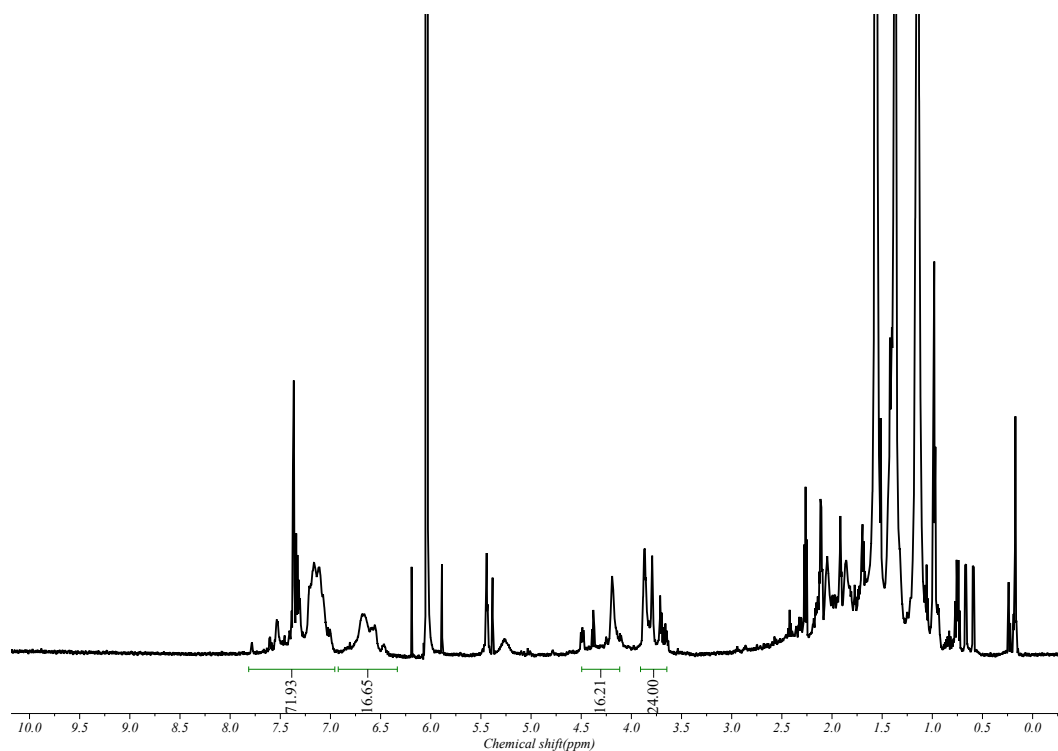
Figure S8. ^{1}H NMR spectra of PPV$_5$-TIPS-b-P2VP$_{15}$ in C$_2$D$_2$Cl$_4$.
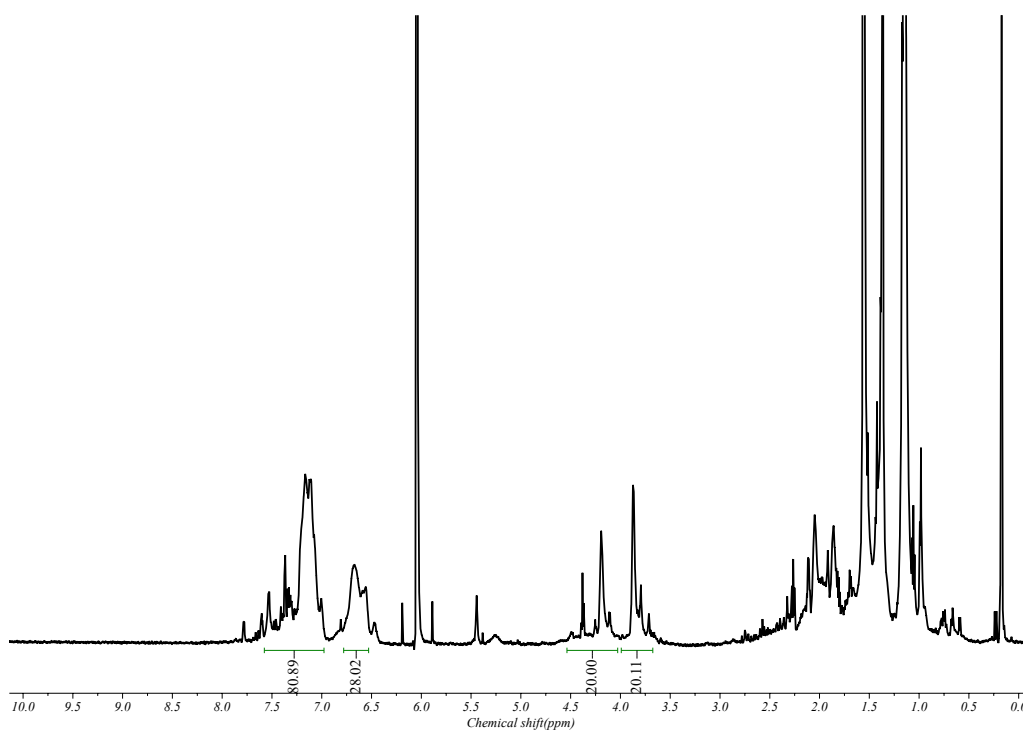
Figure S9. ^{1}H NMR spectra of PPV$_5$-TIPS-b-P2VP$_{20}$ in C$_2$D$_2$Cl$_4$.

Table S2. Summary of the data of ^{1}H NMR and GPC of PPV$_n$-TIPS-b-P2VP$_n$.

BCPs	Retention Time (min)	PDI	Integral of fields of aromatic in ^{1}H NMR (I_a)	Integral of fields of OCH$_2$ in ^{1}H NMR (I_b)	Degree of P2VP polymerization	Block ratio of PPV/P2VP
PPV$_5$-TIPS-b-P2VP$_{10}$	9.28	1.09	68.43	40.33	10	1:2
PPV$_5$-TIPS-b-P2VP$_{15}$	9.02	1.13	88.58	40.21	15	1:3
PPV$_5$-TIPS-b-P2VP$_{20}$	8.81	1.16	108.91	40.11	20	1:4

$$nPPV + nP2VP = \frac{Ia - 8}{4} \qquad \text{(Equation S7)}$$

$$nPPV = \frac{Ib}{8} \qquad \text{(Equation S8)}$$

3. Supporting Figures
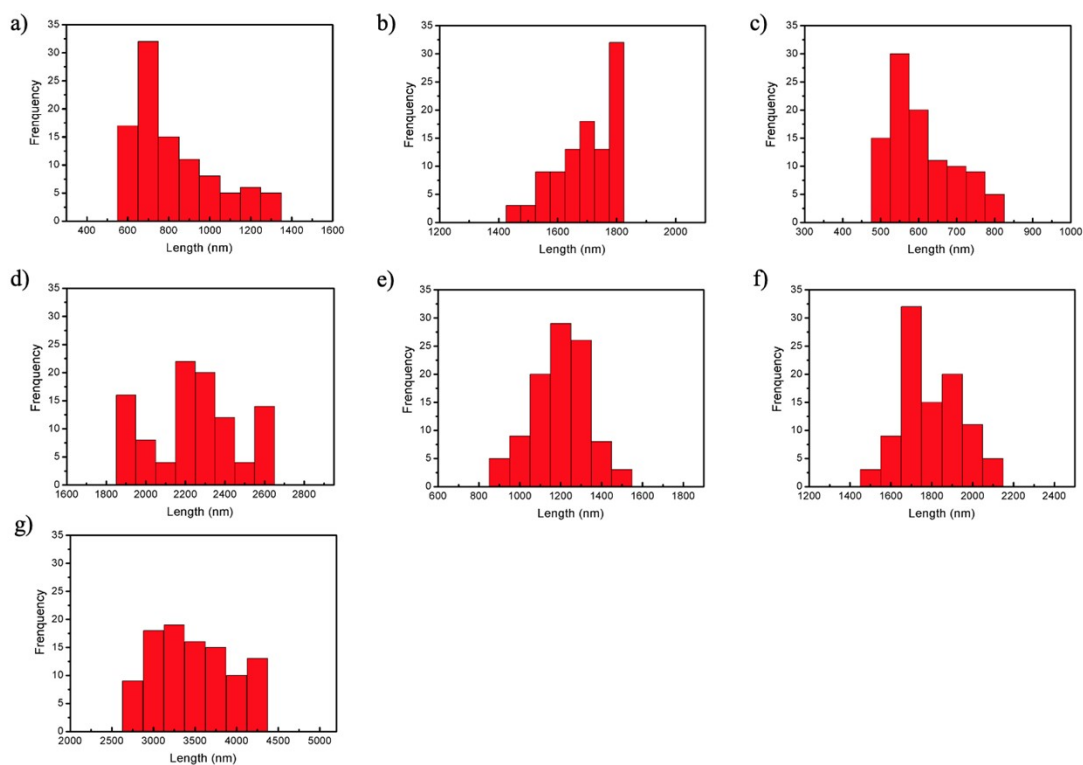
Figure S10. contour length distributions of the number-average length of correspondent micelles formed from PPV_5-TIPS-b-P2VP$_n$ at different concentrations.

a. b. PPV_5-TIPS-b-P2VP$_{10}$ in 0.005 and 0.01 mg ml^{-1} isopropanol solution; **c. d.** PPV_5-TIPS-b-P2VP$_{15}$ in 0.005 and 0.01 mg ml^{-1} isopropanol solution; **e. f. g.** PPV_5-TIPS-b-P2VP$_{20}$ in 0.001, 0.005 and 0.01 mg ml^{-1} isopropanol solution.
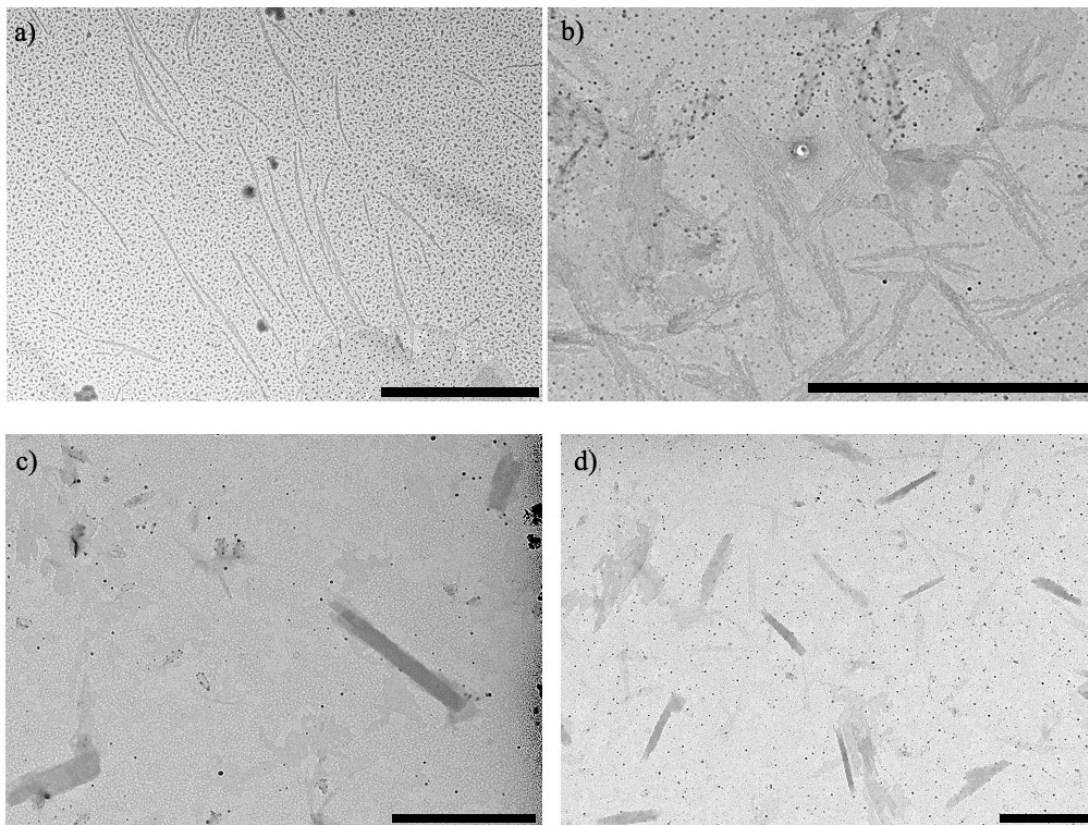
Figure S11. TEM images of growth process of rectangular micelles formed from at 80 °C after aging for (a) 24 h; (b) 36 h; and (c, d) 48 h. Scale bars in TEM photos are 2 µm.
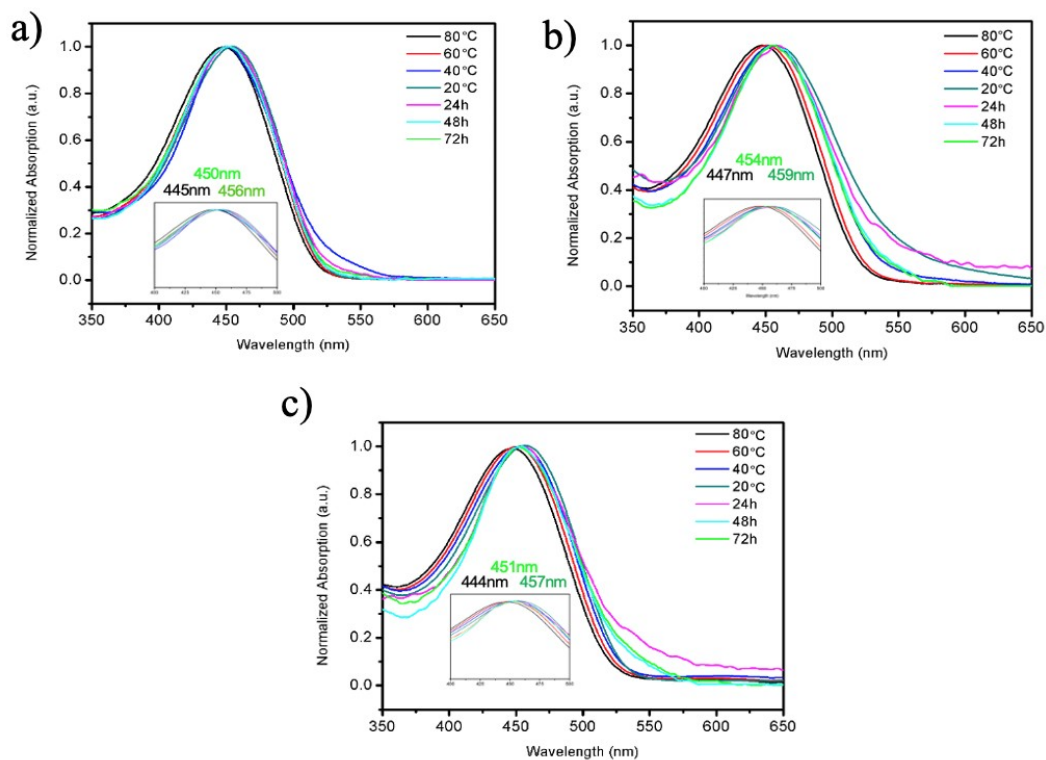
Figure S12. UV-Vis absorption changes of 2D micelles formed from (a-c) PPV_5-TIPS-b-$P2VP_{10}$, PPV_5-TIPS-b-$P2VP_{15}$ and PPV_5-TIPS-b-$P2VP_{20}$ in 0.005 mg ml^{-1} isopropanol solution;
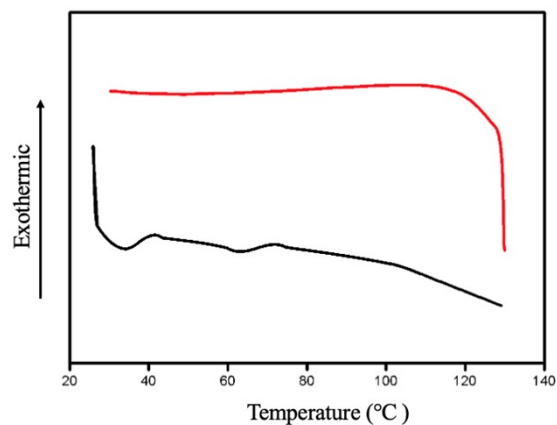
Figure S13. DSC curves of PPV$_5$-TIPS-CHO. The measurements were carried under N$_2$ at a heating rate of 10 °C min^{-1} for twice scan, and the represented curves are recorded for the second heating scan.
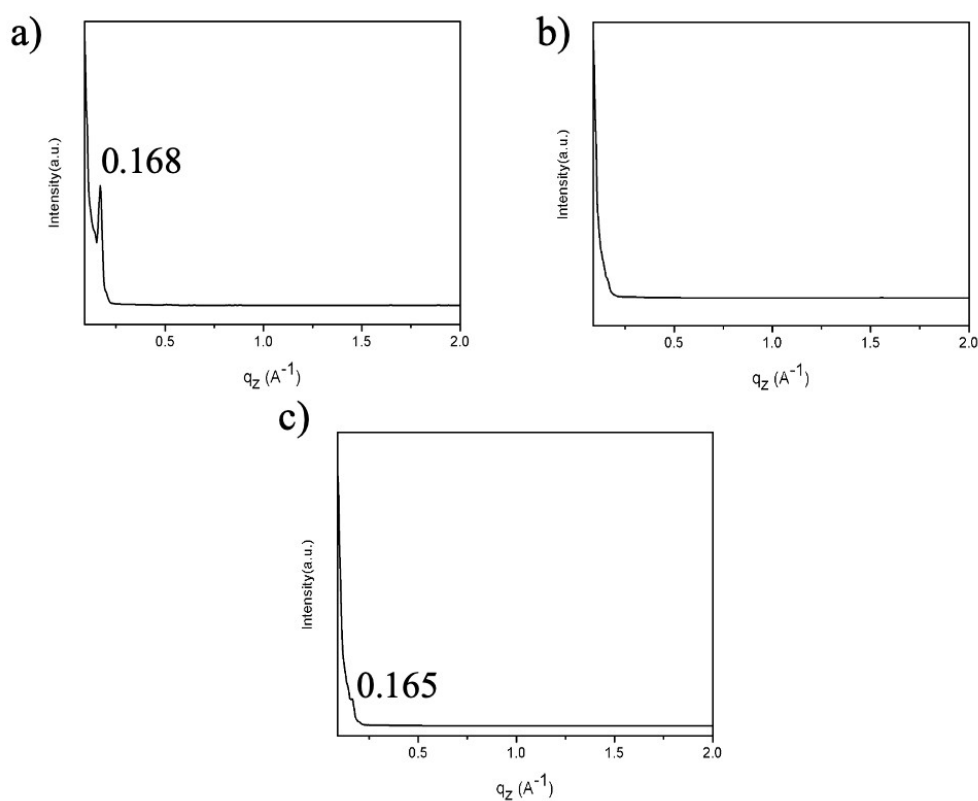

Figure S14. GIWAXS profiles along the out-of-plane direction of platelet 2D square or rectangular micelles obtained from (a) PPV$_5$-TIPS-b-P2VP$_{10}$, (b) PPV$_5$-TIPS-b-P2VP$_{15}$ and (c) PPV$_5$-TIPS-b-P2VP$_{20}$.
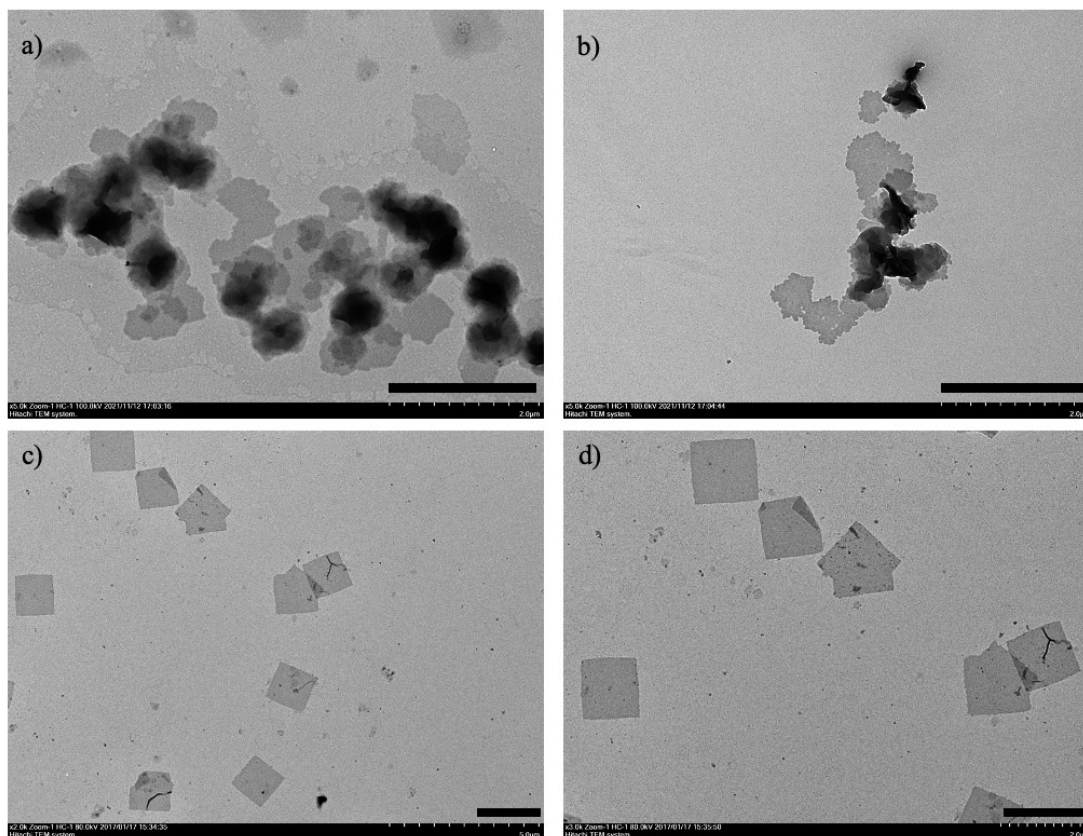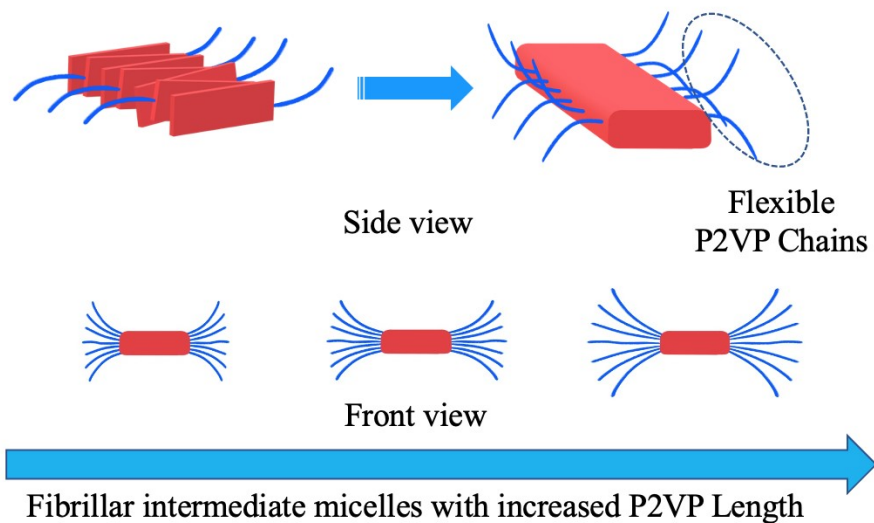
Figure S15. TEM images of (a, b) 2D micelles based on co-assembly with PPV_{12}-*b*-$P2VP_{12}$ and PPV_5-TIPS-*b*-$P2VP_{20}$ at a 0.005 mg·mL^{-1} solution. (c, d) 2D square micelles based on assembly with PPV_{12}-*b*-$P2VP_{12}$ at a 0.005 mg·mL^{-1} solution. Scale bars in TEM photos are 2 μm.
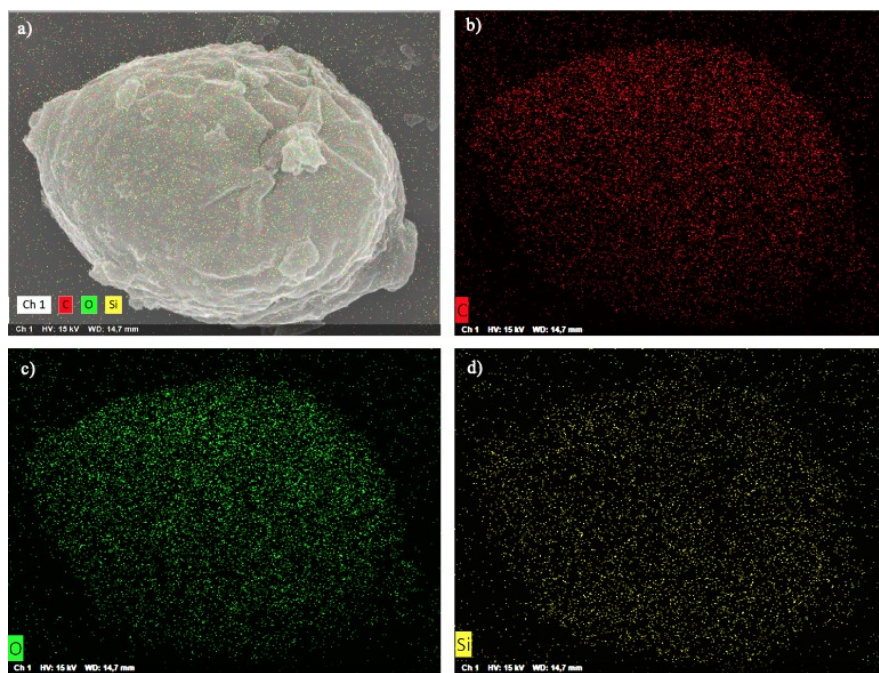
Figure S16. SEM image and corresponding SEM-EDS elemental mapping images of co-assemblies based on EH-PPV-*b*-P2VP and PPV-TIPS-*b*-P2VP at a 0.005 mg·mL^{-1} solution.
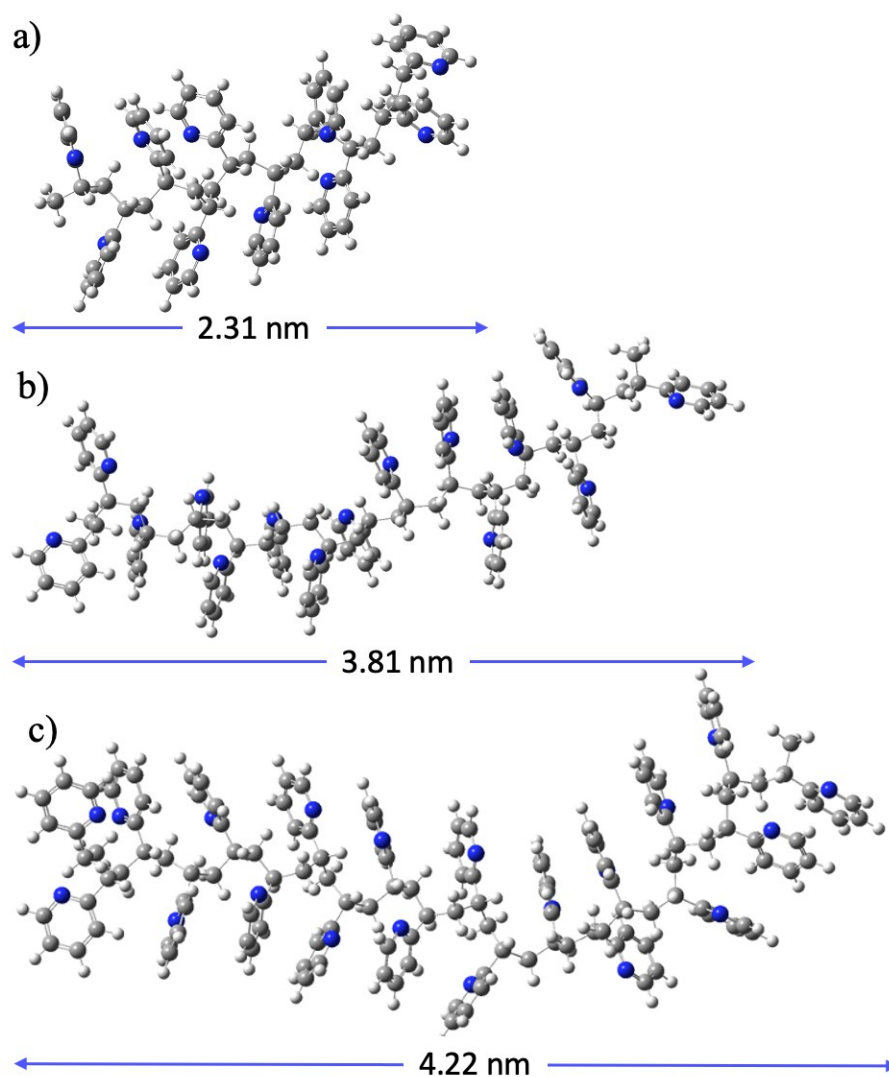
Figure S17. The optimized structures and calculated scales of corona block (a) P2VP$_{10}$, (b) P2VP$_{15}$, and (c) P2VP$_{20}$, respectively, by DFT calculations. The DFT calculations were performed with the Gaussian09 suite of programs. The structure was optimized at the B3LYP level of theory with the 6-31G* basis set.

Figure S18. Schematic diagram of fibrillar intermediate micelles with different block ratios based on the DFT results.
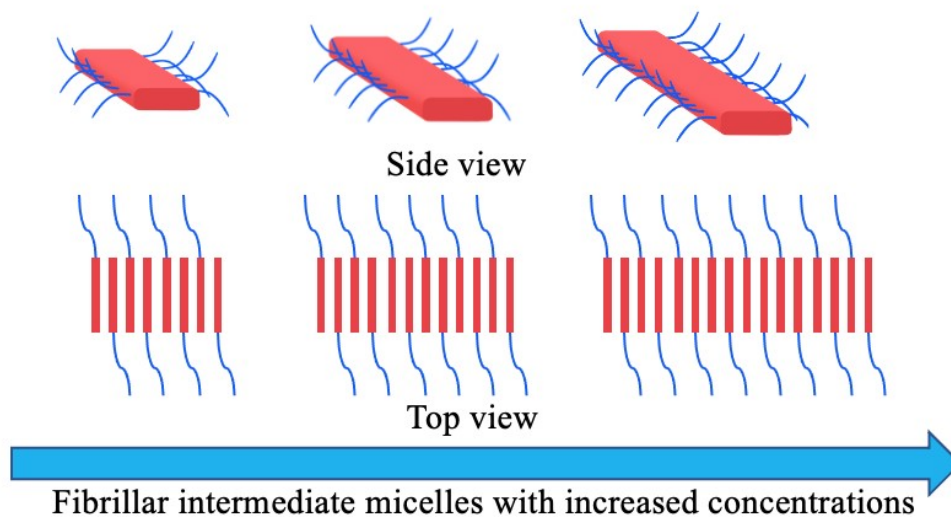
Figure S19. Schematic diagram of the influence of the different concentrations on the fibrillar intermediate micelles formed in the process of preparing the 2D platelets.
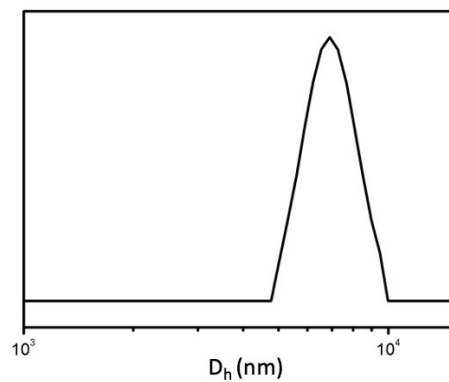
Figure S20. Hydrodynamic diameter (D_h) of 2D nearly circle-like micelles based on co-assembly with PPV_{12}-b-$P2VP_{12}$ and PPV_5-TIPS-b-$P2VP_{10}$ at the 0.005 mg·mL^{-1} solution.